35th Annual International Conference of the IEEE EMBS
Osaka, Japan, 3 - 7 July, 2013

Evaluation of Anomaly Detection Algorithm using Trans-admittance Mammography with 60×60 Electrode Array

Mingkang Zhao, Hun Wi, *Student Member, IEEE,* Tong In Oh*, *Member, IEEE,* and Eung Je Woo, *Senior Member, IEEE*

***Abstract*—Electrical impedance imaging has a potential to detect an early stage of breast cancer due to higher admittivity values compared with those of normal breast tissues. Specially, tumor size and extent of axillary lymph node involvement are important parameters to evaluate the breast cancer survival rate. We applied the anomaly detection algorithm to the high density trans-admittance mammography system for estimating the size and position of breast cancer. We tested 4 different size of anomaly with 3 different conductivity contrasts at 5 different depths. From a frequency difference trans-admittance map, we can readily observe the transversal position and estimate its size and depth. However, the size estimation was dependent on the admittivity contrast between anomaly and background. It requires the robust detection algorithm regardless of the conductivity contrast.**

I. Introduction

Early detection of breast tumor with a favorable prognosis standard method is important to reduce mortality rate. In order to prevent undetected or false predictive case, we have conducted frequent X-ray screening and high number of biopsy to be confirmed. It's very inconvenient and higher risks from ionizing radiation. Electrical impedance imaging has been introduced as an alternative or supplementary method to X-ray mammography because malignant breast tumor tissue has a significantly different electrical impedance spectrum than surrounding normal tissues [1,2]. We may improve sensitivity and specificity using adjunctive technologies in breast cancer detection [3].

Previously, we had developed a trans-admittance scanner with 320 sensing electrodes. It applied a constant voltage with multiple frequencies between a reference electrode on a distal part of a patient and a scan probe placed on the breast to measure exit currents from an array of electrodes inside the probe that were kept at the ground potential [4]. From frequency-difference trans-admittance maps, we tried to estimate the size and depth of tumor to evaluate the breast cancer [5]. However, the scan probe was too much dependent on an operator's skill and error was increased in detecting an anomaly with a small size and large depth.

In order to overcome the hardware limitation of TAS, we developed a high density trans-admittance mammography system recently [6]. It included an array of 60×60 current sensing electrodes with a large solid metal electrode for applying a sinusoidal voltage over a range of frequencies from 50 Hz to 500 kHz. All measured channels were over 70 dB signal to noise ratio at operating frequencies. It had similar structure to X-ray mammography where the breast was situated between two holding plates to integrate both systems easily.

In this study, we evaluated the anomaly detection algorithm with trans-admittance mammography system on a breast phantom. Also, we tested the effect of conductivity contrast between anomaly and background to the depth and size estimation.

II. Method

A. TAM System

Figure 1 describes the measurement configuration and the structure of TAM system. We place the breast between two holding plates like the X-ray mammography. The large top plate of 180×180 mm stainless steel is used to apply a constant sinusoidal voltage to a breast. Same size of bottom plate included 3600 small sensing electrodes is kept at ground potential to produce uniform current density distribution between two plates when it is filled with a homogenous material. Each electrode is plated with gold to stabilize the contact impedance. The diameter of each electrode is 2 mm, and the distance between neighboring electrodes is 3 mm.

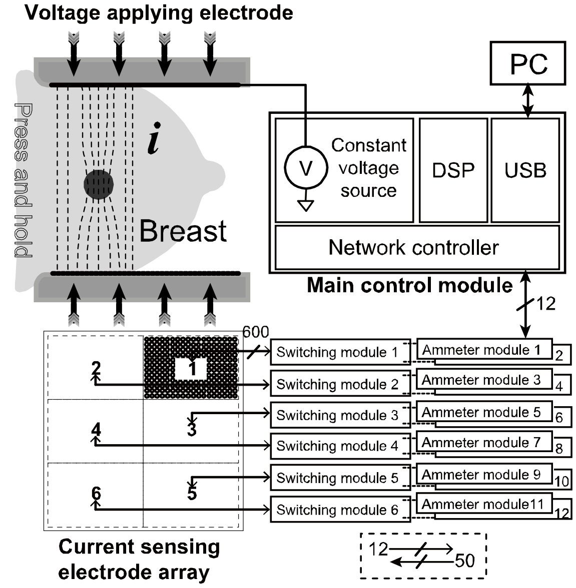

Figure 1. Measurement configuration and structure of TAM system.

Current flows from the voltage applying electrode to each sensing electrodes through the breast tissue because of the potential difference between two plates. We use 12 ammeter modules and 6 switching modules for measuring exit currents

This research was supported by Basic Science Research Program through the National Research Foundation of Korea (NRF) funded by the Ministry of Education, Science and Technology (No. 2011-0022779).

M. Zhao, H. Wi, E. J. Woo and T. I. Oh are with Impedance Imaging Research Center and the Department of Biomedical Engineering, College of Electronics and Information, Kyung Hee University, Yongin-si, Gyeonggi-do 446-701, Korea (phone: +82-31-201-3727; fax: +82-31-201-2378; e-mail: tioh@ khu.ac.kr)

from 3600 sensing electrodes instead of one ammeter for each electrode. To obtain a trans-admittance map at the single frequency, it requires 50 different switching connections. Any conductive anomaly underneath the sensing electrode array can distort the current flow. From the perturbation in the trans-admittance map, we detect the anomaly and analysis the data to estimate position and size. Figure 2 shows developed TAM system included 60×60 sensing electrode array.

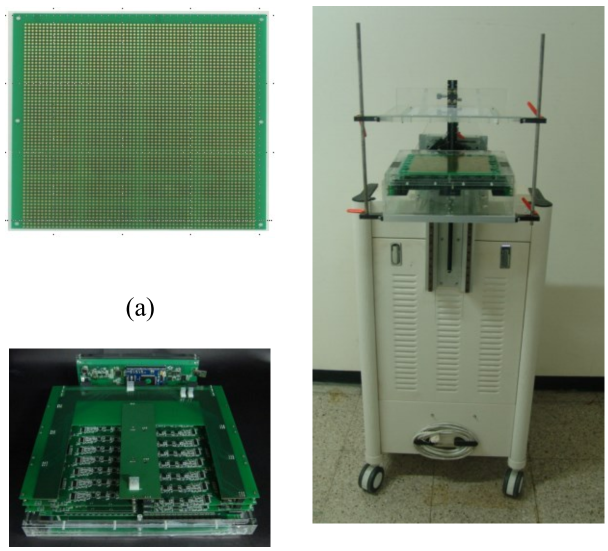

(a) (b) (c)

Figure 2. (a) 60×60 sensing electrode array, (b) bottom view of TAM system and (c) TAM system for human experiment.

B. Anomaly Detection Algorithm

Seo et al developed a mathematical framework and suggested the non-iterative algorithm to extract the position and size of lesions from frequency difference trans-admittance map acquired at multiple frequencies [7-9]. We adopted this algorithm and implemented to the TAM system for estimating the core features of anomaly.

We considered the three-dimensional domain, Ω, of breast bounded by its surface, $\partial\Omega$. We apply a constant voltage of A volt with an angular frequency ω to the large voltage applying electrode plate with contact area, Γ_S. On the opposite side, 3600 current sensing electrodes are kept at ground potential with a total contact area of Γ_M.The electric field between the plates is $V(\mathbf{r})$ at position $\mathbf{r}=(x,y,z)$ inside domain. This satisfied the following mixed boundary condition.

$$\begin{cases} \nabla\cdot\left((\sigma+i\omega\epsilon)\nabla V(\mathbf{r})\right)=0, & \mathbf{r}\in\Omega \\ V(\mathbf{r})=0, & \mathbf{r}\in\Gamma_M \\ V(\mathbf{r})=A, & \mathbf{r}\in\Gamma_S \\ (\sigma+i\omega\epsilon)\nabla V(\mathbf{r})\cdot\mathbf{n}(\mathbf{r})=0, & \mathbf{r}\in\partial\Omega\backslash(\Gamma_M\cup\Gamma_S) \end{cases}$$

When $\mathbf{n}$ is the unit outward normal vector to the boundary, $\sigma=\sigma(\mathbf{r},\omega)$ is the conductivity and $\epsilon=\epsilon(\mathbf{r},\omega)$ is the permittivity. Both of them depend on the position, $\mathbf{r}$ and frequency, ω. In order to detect a lesion underneath the current sensing electrodes, we measure the distribution of exit currents through $\Gamma_M$as

$$-g(\mathbf{r})=\mathbf{n}\cdot(\sigma\nabla v-\omega\epsilon\nabla h)+i\,\mathbf{n}\cdot(\sigma\nabla h+\omega\epsilon\nabla v),\mathbf{r}\in\Gamma_M$$

Where v and $h$are the real and imaginary part of V. It described the relationship between the complex conductivity and the frequency difference trans-admittance map.

We modified the algorithm to match with TAM system with 3600 sensing electrodes. It can provide real and imaginary components of admittance map within 50 Hz to 500 kHz frequency range. Let define $\mathbf{x}^j=(x_1^j,x_2^j)$as the center of j-th electrode, and $F(j)$ as the weighted difference of the trans-admittance map at j-th electrode:

$$F(j)=Im(g_{\omega2}-\alpha g_{\omega1})(\mathbf{x}^j), j=1,\cdots,N.(N=3600).$$

In the anomaly detection algorithm, the first step is to find the transversal position $(\xi_1,\xi_2)$of anomaly.

1 Find index j_0 where the weighted frequency difference current has its maximum value, $F(j_0)=\sup_j F(j)$.

2 Find $j_1,\cdots j_8$, eight neighboring sensing electrodes are of j_0.

3 Calculate (ξ_1,ξ_2):

$$(\xi_1,\xi_2)=\left(1-\sum_{k=1}^{8}\lambda_j\right)\mathbf{x}^{j_0}+\sum_{k=1}^{8}\lambda_k\,\mathbf{x}^{j_k}$$

Where $\lambda_k=\frac{|F(j_k)|}{a+\sum_{k=0}^{8}|F(j_k)|}$

We determine depth $\xi_3$as the second step.

1 Choose a data set A from whole data set $F(j)$

$$A=\{j\ :\ \theta_1F(j_0)<F(j)<\theta_2F(j_0)\}$$

where $0<\theta_1<0.5<\theta_2<1$.

2 For each $j\in A$, compute z_j with $0<z_j<30mm$ satisfying

$$\frac{1}{F(j_0)}\frac{2z_j^2-r_{j_0}^2}{\left(z_j^2+r_{j_0}^2\right)^{5/2}}=\frac{1}{F(j)}\frac{2z_j^2-r_j^2}{\left(z_j^2+r_j^2\right)^{5/2}}$$

Where $r^j=\left|\mathbf{x}^j-(\xi_1,\xi_2)\right|$

3 Calculate the depth ξ_3 using

$$\xi_3=\frac{1}{\sum_{j\in A}F(j)^{-1}}\sum_{j\in A}F(j)^{-1}z_j$$

The third step is determining the size D.

$$\frac{1}{2}\zeta(g_2-\alpha g_1)(x_1,x_2) \approx \beta\left(\frac{\sigma_c}{\sigma_n}-\frac{\kappa_c\epsilon_c}{\kappa_n\epsilon_n}\right) \times|D|\frac{2\varepsilon_3^2-(x_1-\xi_1)^2-(x_2-\xi_2)^2}{4\pi[\varepsilon_3^2+(x_1-\xi_1)^2+(x_2-\xi_2)^2]^{5/2}}$$

Where$\beta=\frac{\omega_2\kappa_n\epsilon_n}{\sigma_n}\frac{(3\sigma_c)^2}{(2\sigma_c+\sigma_n)^2}g_0(\xi_1,\xi_2)$and

$$\sigma=\begin{cases}\sigma_n\ in\ \Omega_L\backslash\bar{D}\\ \sigma_n\ in\ D\end{cases}\ \text{and}\ \epsilon=\begin{cases}\epsilon_n\ in\ \Omega_L\backslash\bar{D}\\ \epsilon_n\ in\ D\end{cases}$$

We choose the D value which has minimum error in the upper equation.

We simulated trans-admittance maps with 3 different size (1, 3.375, 8 cm^3) of cubic anomaly placed inside saline using COMSOL. The depth estimation also follows the trend of real depth. Average error of depth (ξ_3) was 12.66%.

TABLE I. SIMULATION RESULT FOR DEPTH

True		Reconstruction	
Depth (ξ_3)	Size (mm3)	ξ_3	Error (%)
20	3.375	17.8	11
15	3.375	13.24	11.72
20	1	17034	13.3
15	1	12.81	14.6

III. RESULT

In order to evaluate the anomaly detection algorithm and the detection capability of TAM system, we placed a cubic carrot in the saline tank as shown in figure 3. It described the definition of anomaly position, size and depth while TABLE II and III explained the parameter of each volume and depth with estimation values individually. Each length of cuboids was 9, 12, 15 and 18, respectively. Also, we prepared 3 different saline phantoms.

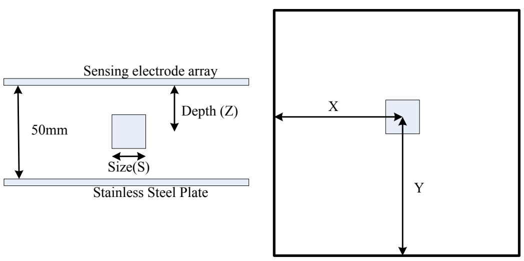

Figure 3. Definition of anomaly size, depth and transversal position.

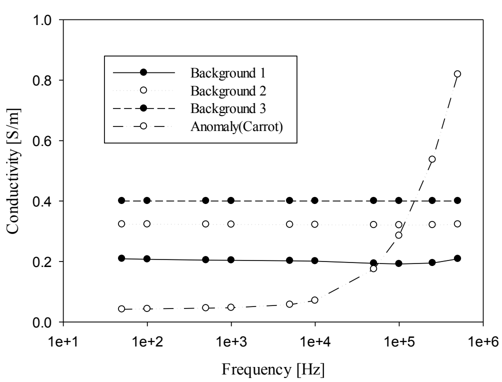

Figure 4. Conductivity spectrum of anomaly and background.

Conductivity spectra of carrot and saline are shown in figure 4. Each saline had a constant conductivity of 0.21(conductivity contrast = 5 times), 0.32 (8 times) and 0.41(10 times)S/m within the operating frequency range. We produced trans-admittance maps with different volume and depth of anomaly. Figure 5 shows an example of imaginary part trans-admittance maps for a carrot of 18 mm^3 at 10 mm depth. We repeated measurements as following with TABLE II. In X-Y plane, we always placed anomaly at X=90mm, Y=100mm position.

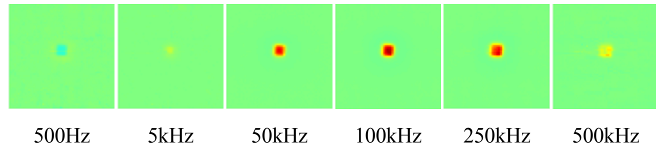

Figure 5. An example of imaginary part trans-admittance map for carrot of 18 mm^3 at 10mm depth.

TABLE II. ESTIMATED DEPTH RESULTS

Real Volume [mm^3]	Real Depth(Z) [mm]	Estimated Depth(Z) [mm]		
		Conductivity ratio: 5	Conductivity ratio: 8	Conductivity ratio: 10
729	5	5.57	7.08	4.43
	10	9.65	8.54	9.00
	15	12.81	12.82	13.13
	20	19.09	15.67	19.57
	25	21.64	19.92	24.64
1728	10	8.98	8.95	9.69
	15	12.09	11.58	13.64
	20	15.06	16.10	17.46
	25	18.50	18.73	25.76
3375	10	10.01	11.65	9.21
	15	12.09	12.25	12.24
	20	15.32	15.29	15.76
	25	20.27	20.29	20.34
5832	10	12.67	11.65	11.63
	15	14.23	12.28	13.43
	20	17.22	15.57	15.97
	25	20.24	19.81	20.85

TABLE III. ESTIMATED VOLUME RESULTS

Real Volume [mm^3]	Real Depth(Z) [mm]	Estimated Volume [mm^3]		
		Conductivity ratio: 5	Conductivity ratio: 8	Conductivity ratio: 10
729	5	324.3363	948.8746	726.8549
	10	1345.769	742.4275	540.7118
	15	274.4297	472.6806	684.3566
	20	944.0454	1000.809	441.6333
	25*	1389.647	7870.901	709.2242
1728	10	3458.319	1433.443	1308.655
	15	1469.22	798.9397	1438.576
	20	942.748	2013.073	579.8977
	25*	2483.473	21329.79	1135.711
3375	10	4585.333	3221.631	2224.931
	15	2658.741	1488.623	2305.99
	20	1611.034	2699.204	995.8527

	25*	8173.132	29365.14	1508.786
5832	10**	12110.55	4756.607	4620.703
	15	5244.694	2946.603	5718.407
	20	3137.398	6103.642	1691.891
	25*	9904.155	54170.93	2640.681

*: Error was increased when anomaly was placed below 20mm depth.
**: In this case, the anomaly is too close to sensing array, estimation error also increase.

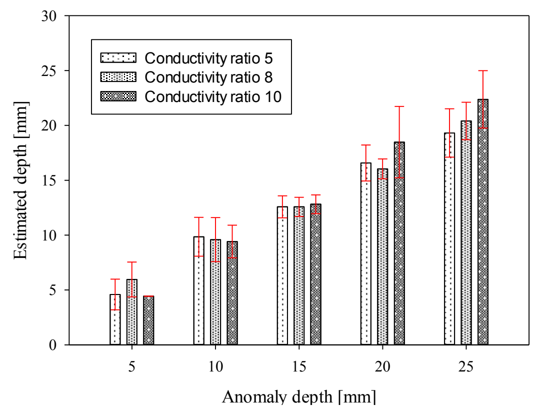

Figure 6. Estimated depth of anomalies with different conductivity ratio to the background saline

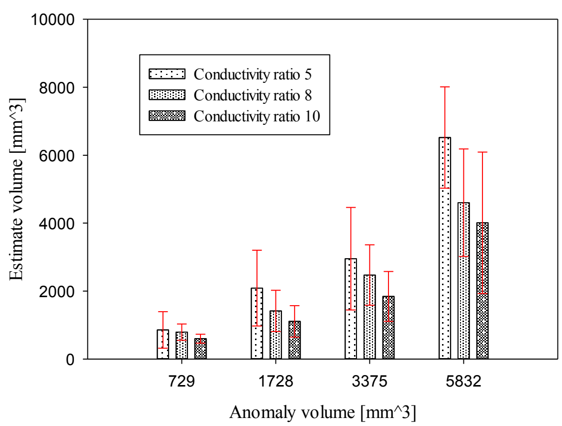

Figure 7. Estimated volume of anomalies with different conductivity ratio to the background saline

After we collected data at each experimental setup, we estimated the anomaly size and depth for each case using the described algorithm. The estimated averaging depth for each case was 4.43, 9.41, 12.81, 18.48, and 22.37mm, respectively. The standard deviation of estimated depth was 1.56 mm among different conductivity cases. Figure 6 shows the mean and standard deviation for each depth with the different conductivity ratio.

We calculated the volume estimation of anomaly using least square estimation method in TABLE III. Figure 7 shows the mean and standard deviation of the volume estimation for each case. The estimated volume were 748, 1538, 2421 and 5044 mm^3 while the real volume were 729, 1728, 3375 and 5825 mm^3.The average standard deviations were 303 mm^3, 728 mm^3, 1044 mm^3, and 1719 mm^3 among different conductivity ratios.

IV. Conclusion and Discussion

We evaluated the anomaly detection algorithm with high density trans-admittance mammography system included 60×60 sensing electrode array. As shown in figure 6, the depth was estimated well within 20 mm. However, error was increased when depth was over 20 mm. The volume estimation was related to the conductivity ratio between the anomaly and background, as shown in figure 7. Compare with the simulation case, these saline experiment estimation shows higher error since the saline experiment data contains more noise and conductivity contrast effect. However, the estimation results from saline experiments show the feasibility of detecting breast tumor using TAM frequency difference image. This anomaly detection algorithm was highly depended on conductivity contrast when estimating volume. It is required to develop a new algorithm which is robust of conductivity contrast between anomaly and background. Also, we can use some prior knowledge of cancerous tissues in conductivity spectrum to improve the depth and volume estimation. For future works, we also plan to test our TAM system on a complex breast model before starting clinical experiment.

References

[1] Surowiec AJ, Stuchly SS, Barr JR, Swarup A, “Dielectric properties of breast carcinoma and the surroundingtissues,”*IEEE Trans Biomed Eng*vol. 35 pp. 257-263, 1998.
[2] Silva JE, Marques JP, Jossinet J, “Classification of breast tissue by electrical impedance spectroscopy,”*Med BiolEngComput*vol. 38 pp. 26-30, 2000.
[3] Malich A, Boehm T, Facius M, FreesmeyerM G, Fleck M, Anderson R, Kaiser W A, “Differentiation of Mammographically Suspicious Lesions: Evaluation of Breast Ultrasound, MRI Mammography and Electrical Impedance Scanning as Adjunctive Technologies in Breast Cancer Detection,” *Clinical Radiology*, vol. 56, pp. 278–283, 2001.
[4] Oh T I, Lee J, Seo J K, Kim S W, Woo E J, “Feasibility of breast cancer lesion detection using a multi-frequency trans-admittance scanner (TAS) with 10 Hz to 500kHz bandwidth,” *Physiol. Meas*., vol.28, pp. S71-S84, 2007.
[5] Christine L. Carter, Carol Allen, Donald E. Henson, “Relation of tumor size, lymph node status, and survival in 24,740 breast cancer cases” , *Cancer , vol. 63, no. 1, pp. 181-187, 1989*
[6] Zhao M, Wi H, Kamal A H M, McEwan A L, Woo E J, Oh T I, “High density trans-admittance mammography development and preliminary phantom tests,”*Biomed EngOnLine*, 11:75, 2012.
[7] Seo J K, Kwon O, Ammari H, Woo E J, “Mathematical framework and anomaly estimation algorithm forbreast cancer detection: electrical impedance technique using TS2000 configuration,”*IEEE Trans. Biomed.Eng.,*vol.51, pp. 1898–906, 2004.
[8] Kim S, Lee J, Seo JK, Woo EJ, Zribi H, “Multi-frequency trans-admittance scanner: mathematical framework and feasibility,”*SIAM J Appl Math*,vol. 69, pp. 22-36, 2008.
[9] Kim S,“Assessment of breast tumor size in electrical impedance scanning,” *Inverse Problems*, vol. 28, pp. 1-13, 2012.